J Radioanal Nucl Chem (2017) 314:1803–1812
https://doi.org/10.1007/s10967-017-5575-5

$^{18}O(p,p'\gamma)^{18}O$ nuclear reaction in the determination of oxygen by proton induced γ-ray emission

Y. Sunitha[1] · **Sanjiv Kumar**[2]

Received: 19 July 2017 / Published online: 31 October 2017

Abstract A particle induced γ-ray emission methodology employing the $^{18}O(p,p'\gamma)^{18}O$ ($E_\gamma = 1982$ keV) nuclear reaction is described for the non-destructive determination of bulk oxygen in materials. The development of the methodology follows a comprehensive measurement of the thick target yields of the 1982 keV prompt γ-rays in the 3.0–4.2 MeV proton energy region and a systematic assessment of such analytical features as the limit of detection, probing depth, precision and accuracy. The methodology is validated by analyzing binary, ternary and multinary oxides. It is simple and rapid, and in combination with prompt γ-ray producing reactions involving the other constituents, enables the complete compositional analysis of oxygen bearing materials.

Keywords PIGE · Oxygen · Atomic composition

Introduction

The determination of oxygen has long been a subject of interest due to the profound influence of the element on the properties of materials [1, 2]. The materials can be thin films or bulk compounds wherein oxygen prevails either as a major constituent or as an impurity element. Amongst the several different methods of oxygen determination, ion beam analysis (IBA) holds an important position by virtue of its non-destructive nature and versatility. An account of the capabilities of IBA for oxygen determination is exquisitely presented in a review article published by Cohen and Rose in early 90s [3]. The IBA methods, by taking cognizance of their probing depths, can be subsumed into two broad categories: those suitable for the determination of surface oxygen and those applicable for 'bulk' oxygen determination. Techniques such as nuclear reaction analysis (NRA), Rutherford backscattering spectrometry (RBS) and 3.05 MeV $^{16}O(\alpha,\alpha)^{16}O$ resonant scattering have a probing depth of a few microns and, therefore, have been extensively used for the determination of oxygen in films and in the surface regions of bulk materials [4–6]. In fact, $^{16}O(\alpha,\alpha)^{16}O$ resonant scattering with a detection sensitivity of $\sim$ 1 at% and a depth resolution of $\sim$ 30 nm, is the most popular method of depth profiling oxygen in materials [7]. Methods based on particle induced γ-ray emission (PIGE), on the other hand, have probing depths up to several tens of μm and therefore provide the determination of 'bulk oxygen' in materials. But the instances of the applications of these methods are far and few. In probably one of the most exemplary applications, Vickridge et al. used PIGE for the precise determination of oxygen in high temperature superconductors. In fact, the measurement was accomplished by the $^{16}O(d,p\gamma)^{17}O$ nuclear reaction ($E_\gamma = 871$ keV) and therefore, the authors referred to the method as the deuteron induced gamma emission (DIGME) technique [8, 9]. The other PIGE methods of oxygen determination utilize the $^{16}O(p,p'\gamma)^{16}O$ ($E_\gamma = 6.1$, 6.9 and 7.1 MeV) and $^{18}O(p,\alpha\gamma)^{15}N$ ($E_\gamma = 5.2$ MeV) nuclear reactions [10–12].

The objective of the present study is to standardize a simple and an easily adaptable PIGE methodology for the routine determination of bulk oxygen in materials which, as stated earlier, has not received much attention despite its

✉ Y. Sunitha
sunibarc@gmail.com

[1] National Centre for Compositional Characterization of Materials, BARC, ECIL Post, Hyderabad 500062, India

[2] Homi Bhabha National Institute, Training School Complex, Anushakti Nagar, Mumbai 400094, India

immense importance. The $^{16}O(d,p\gamma)^{17}O$ nuclear reaction, though possessing excellent analytical attributes, has limited applicability in view of the fact that deuterons are prolific neutron producers and laboratories operating deuteron beams must have adequate shielding against neutrons. The $^{16}O(p,p'\gamma)^{16}O$ nuclear reaction, on the other hand, has several limitations. For example, (a) it occurs only above 6.8 MeV proton energy which precludes the use of low energy accelerators and (b) it suffers nuclear interference from $^{19}F(p,\alpha\gamma)^{16}O$, one of the most sensitive nuclear reactions for fluorine [10]. The likelihood of a significant neutron production at 6.8 MeV or higher proton energy from nuclear reactions involving the other constituents of the target is yet another drawback of the method. Therefore, the $^{16}O(p,p'\gamma)^{16}O$ nuclear reaction is not a favourable choice for routine applications.

The $^{18}O(p,p'\gamma)^{18}O$ nuclear reaction that emits 1982 keV γ-rays, offers an alternate method of bulk oxygen determination using low energy accelerators. Although the thick target yields of the γ-rays have been measured on a few occasions, the analytical capability of the reaction has not been comprehensively probed [10, 13]. Presently, continuing our endeavor to devise simple yet effective methodologies for oxygen determination, we have carried out a systematic investigation on the analytical potential of the $^{18}O(p,p'\gamma)^{18}O$ nuclear reaction which involved (a) the measurement of thick target yields of 1982 keV γ-rays in the 3.0–4.2 MeV proton energy range, (b) an assessment of analytical features such as limit of detection and probing depth and (c) the identification of sources of interferences. The applicability of the method was evaluated by analyzing several binary, ternary and multinary oxides. The compounds examined included lithium titanate and lithium iron phosphate which are important energy materials. It is shown that with the feasibility of oxygen determination, PIGE, by virtue of its simultaneous multi-element detection capability can enable the determination of the overall atomic composition of these compounds in a single measurement.

Experimental details

PIGE measurements

Target preparation

Calcium carbonate ($CaCO_3$) and several oxides which included silicon dioxide (SiO_2), titanium dioxide (TiO_2), zinc oxide (ZnO) and gadolinium oxide (Gd_2O_3) of known stoichiometry were used as targets. The former four chemicals were of Merck origin whereas the last one was procured from Acros Organics. $CaCO_3$ was used for the measurement of thick target γ-ray yields. $CaCO_3$ also served as a standard for quantifying oxygen while the oxides were used as samples for the validation of the methodology. Subsequently, the method was applied for the analysis of other materials such as zirconium oxide, uranium oxide, tungsten (W) powder and tin sulphide of unknown oxygen content. Incidentally, zirconium oxide powders were synthesized from zircon while uranium oxide was in the form of disc, obtained on sintering a green disc of uranium oxide at 1700 °C in air. So far as W powder is concerned, it was obtained from a fusion research facility while the SnS powder was prepared wet-chemically and was stored in the laboratory ambient for a period of about 6 months before analysis.

In order to ascertain the applicability of the method to the matrices of diverse elemental composition, lithium titanate ($Li_2Ti_2O_4$ and Li_2TiO_3), lithium cobalt oxide ($LiCoO_2$) and lithium iron phosphate ($LiFePO_4$) were also analysed. Li_2TiO_3 and $LiCoO_2$ were of Sigma-Aldrich origin while the other two were from other laboratories: $Li_2Ti_2O_4$ was synthesized by solid-state reaction route while $LiFePO_4$ was prepared by a surfactant based sol–gel approach. Since the complete compositional analysis of the materials is one of the objectives of the study, lithium carbonate (Li_2CO_3) (Qualigens), cobalt carbonate ($CoCO_3$), potassium dihydrogen phosphate (KH_2PO_4) (s d fine chemicals) were used as the standards of Li, Co and P respectively while single crystals of Si (Semiconductor Wafer Inc.) and high purity (> 99.5%) foils (thickness $\leq$ 0.5 mm) of Ti, Fe and Zr (Alfa Aesar) were used as the standards of the respective elements. The single crystal of Si was etched in HF medium while the foils were abraded under argon atmosphere before loading them in the scattering chamber in order to remove the layers of native oxide.

The compounds were in powder form. The purity of the materials used as standard or for validation was better than 99.0%. The compounds, prior to measurements, were mixed with 20 wt% high purity graphite powder and pressed into 10–20 mm circular discs (thickness $\sim$ 1 mm) to serve as targets. The homogeneity of the mixtures was ascertained by measuring the yields of 1982 keV γ-rays at a particular proton beam energy at different locations on the targets.

Irradiation and γ-ray detection

The PIGE experiments were conducted with a 3.0–4.2 MeV proton beam ($\Phi \sim 3$ mm) obtained from the 3 MV Tandetron (High Voltage Engineering Europa, The Netherlands) at NCCCM, Hyderabad. The specimens of the standard and the samples were fixed on an electrically insulated manipulator mounted on a scattering chamber.

The manipulator was surrounded by a negatively biased secondary electron suppressor for current measurement and charge integration. The chamber was maintained at $\sim 5 \times 10^{-6}$ torr pressure during the experiments which involved the irradiation of the targets at normal incidence with protons of the requisite energy and the detection of the prompt γ-rays by a high purity germanium detector (HPGe) (Bruker Baltic, efficiency: 36%, energy resolution: 1.78 keV at the γ-ray energy of 1332 keV of ^{60}Co) placed in the direction of the beam in air. The detector subtended a solid angle of 0.46 sr and was surrounded by a 2.0 cm thick cylindrical lead shield.

Depending on the nature of the matrix, the proton beam current during irradiation ranged from 3 to 50 nA; the lighter matrices were irradiated with lower beam currents while the heavier matrices, with higher beam currents. The duration of the measurements varied accordingly; it ranged from ~ 45 (heavier matrices) to ~ 90 min (light matrices). The data was acquired on a PC based 8 K multichannel analyzer.

Quantification

The content of oxygen or the atomic composition of a material was determined by the relative method. A binary oxide can be represented by a general formula A_xO_y where A is an element and $x + y = 1$. The atomic ratio i.e. x/y in the binary oxides was determined using the following formula that was derived from the standard thick-target yield equation [14]:

$$\frac{x}{y} = \frac{C_{\mathrm{A(std)}} \times R_{\mathrm{A}} \times \varepsilon_{\mathrm{O(std)}}}{C_{\mathrm{O(std)}} \times R_{\mathrm{O}} \times \varepsilon_{\mathrm{A(std)}}} \quad (1)$$

where

$$R_i = \frac{Y_{\mathrm{i(samp)}}}{Y_{\mathrm{i(std)}}}. \quad (2)$$

In Eq. (1) $C_{\mathrm{A(std)}}$ and $C_{\mathrm{O(std)}}$ represent the concentration of element A and oxygen in their respective standards, Y_{i} is the charge-normalised yield of the characteristic γ-rays of the element i (A or oxygen) in the sample (samp) or standard (std); $\varepsilon_{\mathrm{A(std)}}$ and $\varepsilon_{\mathrm{O(std)}}$ are the stopping cross-sections of the proton in the standards of element A and oxygen respectively. It is worthwhile mentioning that Eq. (1) it is valid for cases wherein the standard of the element A and that of oxygen are two different chemical entities but it can be suitably modified if the same compound serves as the standard for both elements.

It is implicit that the Eq. (1) is applicable for compounds whose constituent A is also sensitive to PIGE (Table 1). However, if this is not the case or there is a lack of a suitable standard of A, it is more appropriate to represent the compound by the formula $A_{1-x}O_x$ and the concentration of oxygen in terms of atomic fraction (i.e. x) can be calculated using the formula

$$x = \frac{(12M\varepsilon_{\mathrm{A}} + NW_{\mathrm{A}}\varepsilon_{\mathrm{C}})}{12M\left(\frac{\varepsilon_{\mathrm{O(std)}}}{R_{\mathrm{O}}C_{\mathrm{O(std)}}} + (\varepsilon_{\mathrm{A}} - \varepsilon_{\mathrm{O}})\right) + N\varepsilon_{\mathrm{C}}(W_{\mathrm{A}} - W_{\mathrm{O}})} \quad (3)$$

where ε_{A} and ε_{O} are the stopping cross-sections of element A and oxygen respectively while M and N represent the weight fractions of compound ($A_{1-x}O_x$) and the graphite in the target respectively. Also, W_{A} and W_{O} are the atomic weights of element A and oxygen respectively.

The ternary (e.g. $LiCoO_2$) or quaternary ($LiFePO_4$) oxides can be represented by chemical formula $A_xB_yO_z$ or $A_xB_yC_zO_p$ where the sum of the atomic fractions of all the elements in a compound is unity. The atomic composition of these compounds can be calculated using formula similar to Eq. (1) which is not mentioned here for the sake of brevity. Importantly, it is presumed that all the constituent elements of the compounds are sensitive to PIGE. The reactions involving these and several other elements relevant to the present study and their characteristic prompt γ-rays are listed in Table 1 for referencing [13]. The stopping cross-sections of the elements and compounds obtained from SRIM-2013 were used in calculations [15].

Table 1 List of nuclear reactions and their respective characteristic prompt γ-rays [13]

Element	Nuclear reaction	Eγ(keV)
Li	^{7}Li(p,p′γ)^{7}Li	478
O	^{18}O(p,p′γ)^{18}O	1982
Si	^{28}Si(p,p′γ)^{28}Si	1779
P	^{31}P(p,p′γ)^{31}P	1266
Ti	^{48}Ti(p,p′γ)^{48}Ti	981
Fe	^{56}Fe(p,p′γ)^{56}Fe	843
Co	^{59}Co(p,p′γ)^{59}Co	338
Zr	^{90}Zr(p,γ)^{91}Nb	1082

Proton elastic backscattering spectrometry (p-EBS)

In addition to PIGE, the specimens of lithium titanate and lithium iron phosphate were also analysed by p-EBS. The experiments were performed with 1.5 or 2.0 MeV protons in another scattering chamber maintained at $\sim 5 \times 10^{-6}$ torr pressure. The samples were in the form of 10 mm diameter discs prepared by pressing the compounds without any additive i.e. graphite. The beam diameter was about 1.5 mm while the beam current was about 5 nA. The beam was incident normally on the samples and the backscattered protons were collected by a Si surface barrier

detector positioned at a backward angle of 165 (± 0.3)°. The atomic composition of the compounds was determined by simulating the experimental data using SIMNRA [16]. Since the scattering of 1.5–2.0 MeV protons from lithium, carbon or oxygen is non-Rutherford, the experimentally determined differential cross-sections of ^{6}Li(p,p)^{6}Li, ^{7}Li(p,p)^{7}Li, C(p,p)C and O(p,p)O scatterings were used in the simulations [17–20]. In fact, the cross-sections for the ^{6}Li(p,p)^{6}Li scattering reported in Ref. [17] are for 164° angle but were used for simulations due to the absence of the data for the scattering at 165° angle under the premise that the cross-sections at the two angles are not significantly different. Furthermore, any discrepancy in the overall atomic composition arising from the application of the data at 164° angle is expected to be marginal since the compounds contain Li in natural isotopic abundance. Incidentally, the Rutherford scattering cross-sections for P, Ti and Fe at the relevant energies were used in the simulations.

Results and discussion

Analytical features

Figure 1 shows a typical prompt γ-ray spectrum recorded with the HPGe detector on irradiating the $CaCO_3$ disc with 3.0 MeV proton beam. The 1982 keV γ-rays emitted from the ^{18}O(p,p′γ)^{18}O nuclear reaction are prominently present in the spectrum. The spectrum also contains 495 and 871 keV γ-rays, attributable to the ^{16}O(p,γ)^{17}F ($Q = 0.596$ MeV) and ^{17}O(p,p′γ)^{17}O nuclear reactions respectively. These reactions occur simultaneously with the ^{18}O(p,p′γ)^{18}O reaction during irradiation. It is important to note that the relative natural abundance of the ^{16}O, ^{17}O and

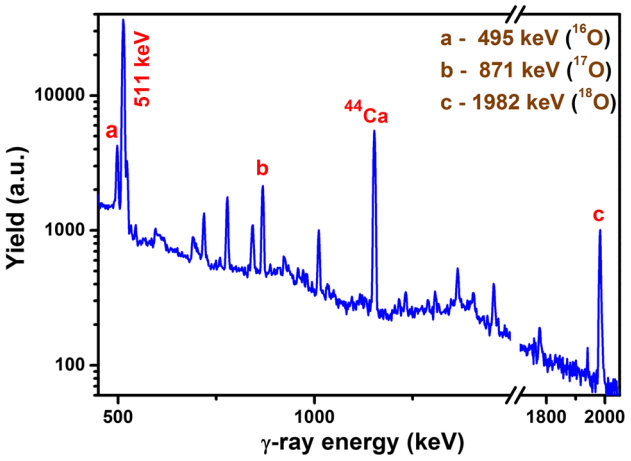

Fig. 1 Prompt γ-ray spectrum of a target consisting of 75 wt% $CaCO_3$ and 25 wt% high purity graphite recorded at 0° with HPGe using a 3 MeV proton beam

^{18}O isotopes is 99.758, 0.037 and 0.204% respectively. A perusal of energy level schemes reported in references [21, 22] shows that the 495 keV γ-ray results from the transition from the first excited state with $J = 1/2^+$ to the ground state with $J = 5/2^+$ of the ^{17}F nucleus; the 871 keV γ-ray, from the first excited state with $J = 1/2^+$ to the ground state with $J = 5/2^+$ of the ^{17}O nucleus while the 1982 keV γ-ray emanates following the transition from the first excited state with $J = 2^+$ to the ground state with $J = 0^+$ of the ^{18}O nucleus.

In order to ascertain the analytical proficiency of these reactions, the thick-target yields of the 495, 871 and 1982 keV γ-rays were measured at 0° as well as 90° angles (with respect to the direction of the beam) in the 3.0–4.2 MeV proton energy range at 200 keV energy intervals. The counts under a γ-ray peak obtained after the subtraction of a linear background were normalized to the total charge and the solid angle of the measurement which served as the yield of the corresponding γ-ray. The yields of the γ-rays measured as a function of beam energy at 0° and 90° angles are shown in Fig. 2 for illustration. The important inferences drawn from the yield measurements are: (a) the yield of the γ-rays, more pronouncedly that of the 1982 keV γ-rays, increases with proton beam energy, (b) amongst the three, the 1982 keV γ-ray has the highest yield above $E_p = 3.6$ MeV and (c) the 495 as well as 871 keV γ-rays have, irrespective of incident beam energy, nearly identical yields at 0° and 90° while the 1982 γ-rays have a comparatively higher yields at the 0° detection angle. The near constancy of the yields of the 495 or 871 keV γ-rays at 0° and 90° angles is consistent with the angular isotropic distribution of γ-rays emitted as a result of the transition from a $J = 1/2^+$ state.

Figure 2 also shows the limits of detection (LOD) of the nuclear reactions in the calcium carbonate (25 wt%) and graphite (75 wt%) mixture at different bombarding energies and detection angles. The LODs are calculated on the basis of three times the standard deviation of the background under the relevant γ-ray peaks. These follow the trend witnessed for thick target yields and accordingly, the best LOD of ~ 1.7 at% is obtained for the ^{18}O(p,p′γ)^{18}O nuclear reaction for measurements at 0° angle with the 4.2 MeV proton beam. The LODs of ^{16}O(p,γ)^{17}F and ^{17}O(p,p′γ)^{17}O nuclear reactions, on the other hand, measure about 18 and 14 at% respectively under similar experimental conditions. Therefore ^{18}O(p,p′γ)^{18}O is the most suitable reaction for oxygen determination. The analysis of different materials showed that the LOD of the reaction varies considerably with the nature of the matrix. In materials composed of high Z elements that are not prolific prompt γ-ray emitters (e.g. lanthanides, tungsten, uranium etc.), the ^{18}O(p,p′γ)^{18}O nuclear reaction has a LOD of about 2 at%. Conversely, in materials consisting of

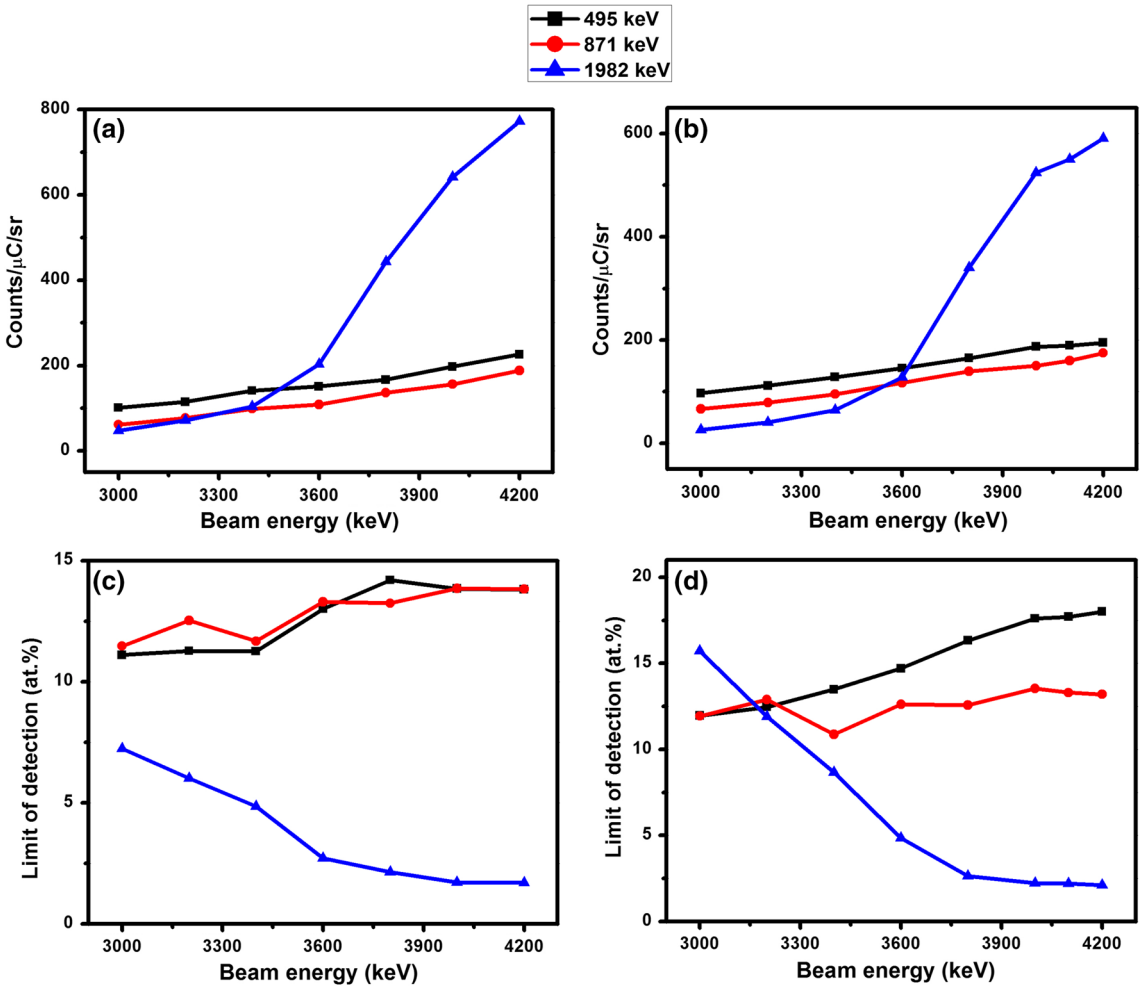

Fig. 2 Thick target yields of the 495, 871 and 1982 keV γ-rays emitted from the $^{16}O(p,\gamma)^{17}F$, $^{17}O(p,p'\gamma)^{17}O$ and $^{18}O(p,p'\gamma)^{18}O$ nuclear reactions at **a** 0° and **b** 90° angles of detection. The curves in **c** and **d** represent the limits of detection of the reactions at 0° and 90° angles of detection respectively

low Z elements which are sensitive to PIGE (e.g. B, Li, Na, Al etc.) the LOD of the reaction is 15–20 at% due to a higher background around 1982 keV in the γ-ray spectra. Notably, for such elements as Al, P and S, the peak of 1982 keV γ-rays is situated on the Compton edge of the 2211, 2230 or 2230 keV γ-rays emitted from the $^{27}Al(p,p'\gamma)^{27}Al$, $^{31}P(p,\gamma)^{32}S$ and $^{32}S(p,p'\gamma)^{32}S$ nuclear reactions respectively. This is well illustrated by the γ-ray spectrum of SnS powder containing oxygen as an impurity in Fig. 3.

Apart from nuclear or spectral interferences, the prevalence of moisture in the compounds can also be a cause of concern, as it may result in an overestimation of their oxygen contents. Presently, though an independent measurement on the content of moisture in the samples was not performed, it, if existing, is presumably removed during the creation of the vacuum. This is manifested in the stability of the targets under proton beam irradiation which is indicated by the constancy of the charge normalized yields

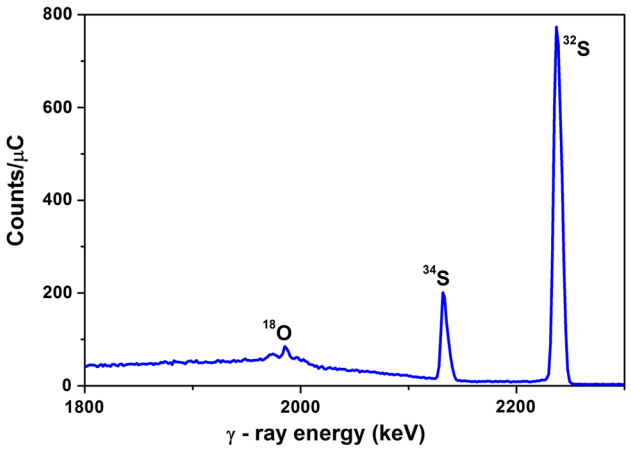

Fig. 3 Prompt γ-ray spectrum of SnS acquired with 4.0 MeV protons

of the 1982 keV γ-rays for repeated measurements. So far as the probing depth is concerned, for the $^{18}O(p,p'\gamma)^{18}O$ reaction it is ∼ 60 μm in SiO_2, ∼ 40 μm in TiO_2

and ~ 30 μm in UO_2 at $E_p = 4.2$ MeV considering that the reaction commences at $E_p = 3.0$ MeV. In view of the rather large probing depth, the method can be conveniently employed for the determination of bulk oxygen in materials.

Validation and analytical results

The analytical efficacy of the $^{18}O(p,p'\gamma)^{18}O$ nuclear reaction was ascertained by analysing several binary oxides with well-defined stoichiometry. Table 2 lists the measured contents of oxygen in some of these oxides along with their theoretical oxygen stoichiometry. The prompt γ-ray spectra of representative oxides of low, mid and high Z elements namely SiO_2, TiO_2 and Gd_2O_3 respectively used for the determination are shown in Fig. 4 for illustration. The spectrum of SiO_2 consists of a strong γ-ray peak at 1779 keV and that of TiO_2, at 981 keV attributable to the $^{28}Si(p,p'\gamma)^{28}Si$ and $^{48}Ti(p,p'\gamma)^{48}Ti$ nuclear reactions respectively. However, gadolinium emits low energy γ-rays and therefore these are not shown in the spectrum. The quantitative analyses of SiO_2 and TiO_2 specimens were carried out using Eq. (1) and, for the sake of comparison, also using Eq. (3) while the content of oxygen in Gd_2O_3 was determined using only Eq. (3) due to the unavailability of a proper standard of gadolinium. It can be observed from Table 2 that the measured contents of oxygen in the first three and also in the other materials are in good (3–7%) agreement with the respective theoretical concentrations. Insofar as the Eqs. (1) and (3) are concerned, the former is expected to yield more accurate results since it utilises standards for both the elements. However, as evidenced by the data in Table 2, both the equations provide nearly identical results. This inference underscores the adequacy of the Eq. (3) for the determination of oxygen in matrices

Table 2 Concentration of oxygen in different binary oxides determined using $^{18}O(p,p'\gamma)^{18}O$ nuclear reaction (triplicate or higher number of measurements)

Oxide	Reference (at%)	Determined (at%)	
		Equation (1)	Equation (3)
Silicon dioxide	66.7	67.3 ± 1.0	65.0 ± 1.5
Titanium oxide	66.7	67.3 ± 1.0	66.5 ± 1.3
Zinc oxide	50.0	–	48.5 ± 1.2
Zirconium oxide[a]	–	68.5 ± 1.2	66.5 ± 1.0
Zirconium oxide[b]	–	66.2 ± 1.0	63.3 ± 1.5
Gadolinium oxide	60.0	–	64.0 ± 1.0
Tungsten powder	–	–	15.7*
Uranium oxide	–	–	62.6 ± 1.0

[a, b] Two different samples of zirconium oxide

* Single measurement

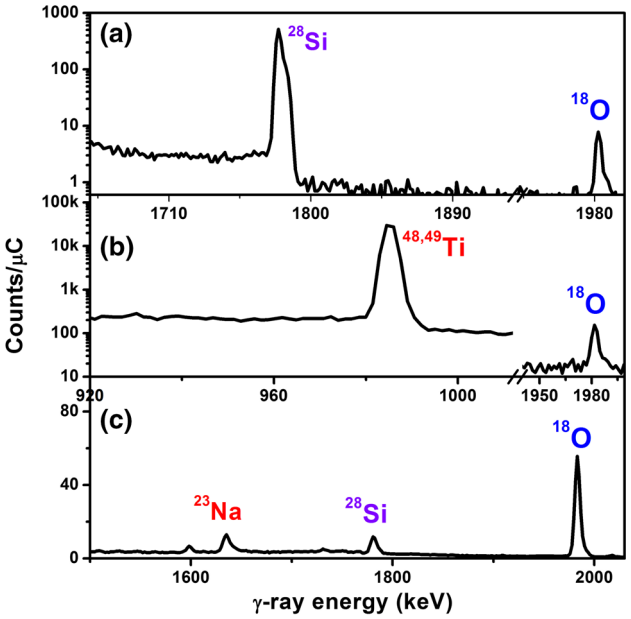

Fig. 4 Prompt γ-ray spectra of **a** SiO_2, **b** TiO_2 and **c** Gd_2O_3 acquired with 4.0 MeV protons respectively

composed of heavy metals, many of which do not produce prompt γ-rays (e.g. Sn, La) in the proton energy range used in the present study. In fact, the absence of strong prompt γ-ray producing reactions facilitates measurements with better precision (~ 1%) in heavier matrices as compared to the precision of ~ 3% observed for the lighter matrices.

The method was utilised to determine oxygen in a sintered disc of uranium oxide (UO_x) and tungsten powders. Figure 5 shows the prompt γ-ray spectra of the two kinds of samples acquired with 4.2 MeV protons wherein the peaks due to the 1982 keV γ-rays are conspicuously present. Uranium does not emit any prompt γ-ray and the 1001 keV γ-ray in the spectrum of uranium oxide has its origin in ^{234m}Pa, a progeny of ^{238}U. Tungsten, on the other hand, emits 101, 111 and 122 keV γ-rays by way of the $^{182}W(p,p'\gamma)^{182}W$, $^{184}W(p,p'\gamma)^{184}W$ and $^{186}W(p,p'\gamma)^{186}W$ nuclear reactions respectively. The 1014 or 1779 keV γ-rays in the spectra are due to minor (~ 1 wt%) impurities of Al and or Si prevailing in the samples. The concentration of oxygen in the two specimens calculated using Eq. (3) is presented in Table 2. It is important to mention that the precision of the oxygen content in the UO_x specimen, estimated on the basis of five measurements with each lasting for about 45 min at a beam current of about 50 nA, is about 1%. The method, therefore, is well suited for the determination of oxygen and, indirectly O/U ratio, in uranium oxide samples with non-destructive analysis, rapidity and insensitivity to uranium oxidation states being the major advantages. So far as the other specimen is concerned, it serves as yet another example to demonstrate the applicability of the method to high Z matrices.

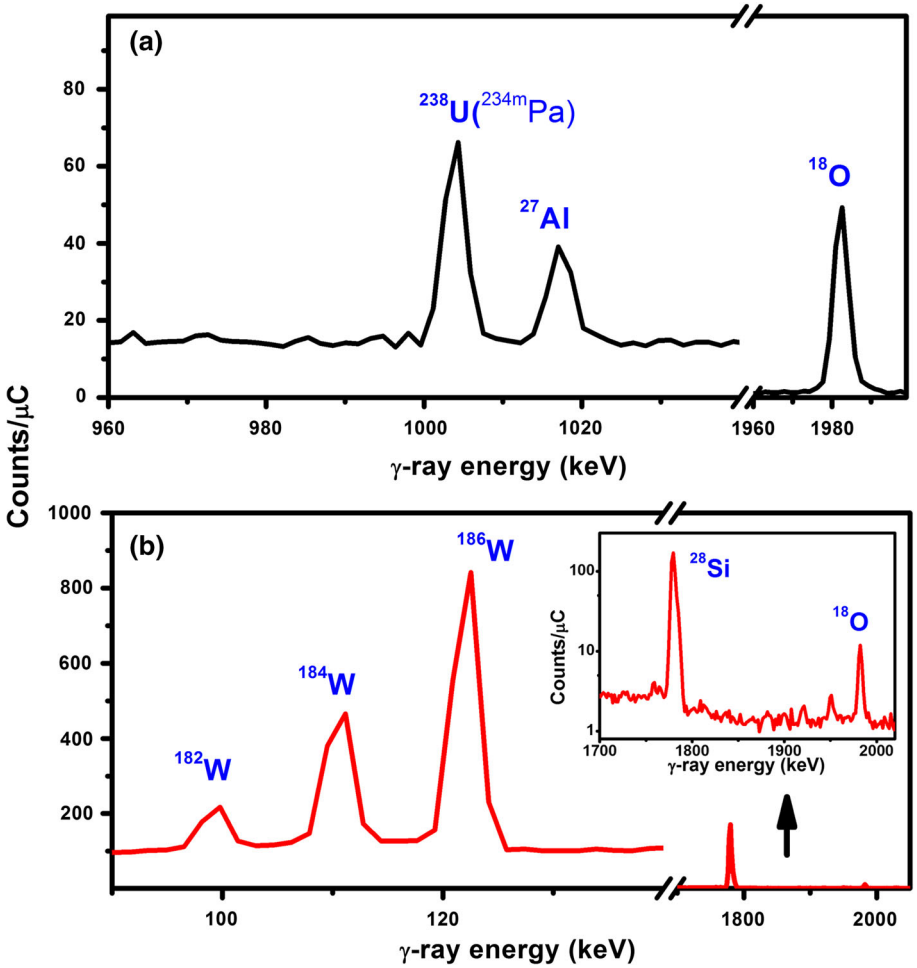

Fig. 5 Prompt γ-ray spectra of **a** uranium oxide and **b** tungsten oxide acquired with 4.2 MeV protons. The inset in fig. **b** shows the peaks of Si and oxygen

Moreover, W powders are extensively used in fusion research and the method can be applied to study oxygen pick up and or its retention during processing.

The method is equally applicable to ternary oxides, namely lithium titanate and lithium cobaltate as well and provides their analysis with reasonably good accuracy and precision. A typical PIGE spectrum of lithium titanate is shown in Fig. 6(a) while the measured atomic compositions of the titanate and cobalate ceramics are presented in Table 3. PIGE exhibits high sensitivity ($\sim$ 10 ppm) to lithium. As a result, the spectrum consists of a very strong peak of the 478 keV γ-rays emitted from the ^{7}Li(p,p′γ)^{7}Li reaction. The higher sensitivity also requires the acquisition of data at a proton beam current of 2-3 nA to keep the dead time within acceptable ($< 5\%$) levels. Furthermore, the peak due to the 1982 keV γ-rays of oxygen is situated on an elevated background caused by the ^{7}Li(p, γ)^{8}Be nuclear reaction that emits 17.6 MeV γ-rays [23]. As a result, the data are collected for a comparatively longer period of time ($\sim$ 90 min) in order to ensure measurements with good statistics.

Lithium titanate and lithium cobaltate are important energy materials but are analytically intractable. It was, therefore, considered worthwhile to the analysis of the titanate ceramics by p-EBS in order to cross-validate the PIGE results. It is important to mention that p-EBS, by virtue of higher cross-sections of the ^{16}O(p,p)^{16}O scattering, has previously been utilised for analysing oxygen bearing materials including high temperature superconductors, for instance yttrium barium copper oxide ($YBa_2Cu_3O_x$) [24, 25]. The spectrum (of $Li_2Ti_2O_4$) shown in Fig. 6(b) represents a typical proton-backscattered spectrum of titanate ceramics wherein the signal of O and also that of Ti/Li are distinctly observed. Notably, as is evident by the superimposed curve, it was simulated satisfactorily for quantification. The data presented in Table 3 show that the backscattering spectrometry technique provides good results too but these are not entirely consistent with the theoretical compositions or those measured by PIGE. Rutherford backscattering spectrometry (RBS) is an absolute method but the accuracy of the method, as described recently by Colaux et al. depends on a number of parameters [26]. p-EBS is analogous to RBS except that the

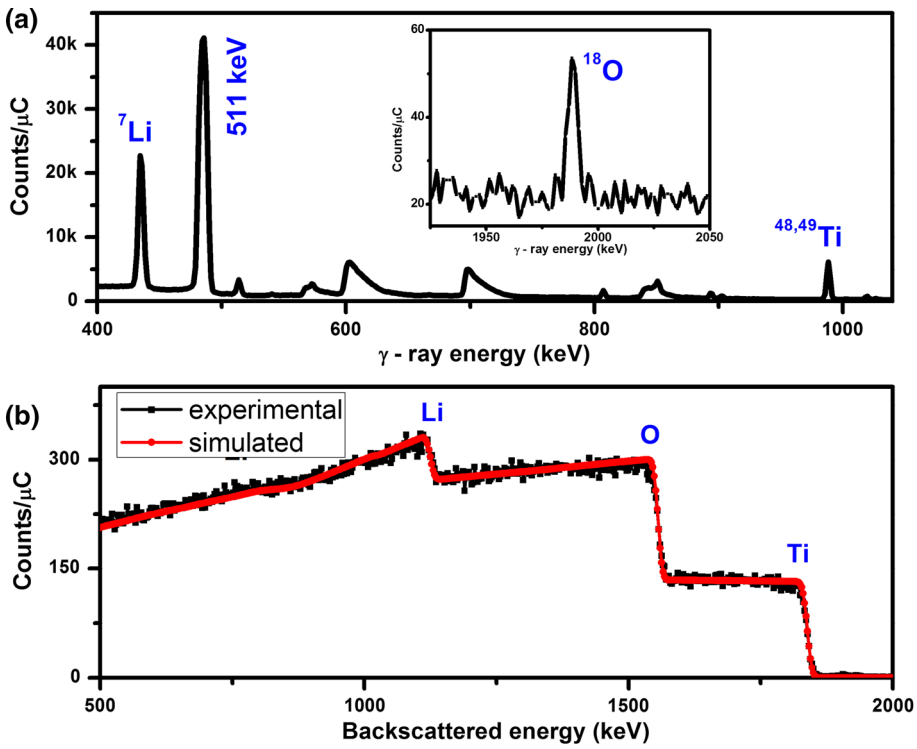

Fig. 6 Analysis of $Li_2Ti_2O_4$: **a** a PIGE spectrum and **b** a proton backscattered spectrum recorded with 4.0 and 2.0 MeV protons respectively. The inset in Fig. **a** shows the peak of oxygen

Table 3 Atomic composition of ternary oxides determined by PIGE and p-BS

Oxide	Chemical formula	Determined [Li:Ti(Co):O]	
		PIGE	P-BS
Lithium titanate	$Li_2Ti_2O_4$	1:1:2.2	1:1.1:2.6
Lithium titanate	Li_2TiO_3	2:1:3.2	2:0.8:3.3
Lithium cobaltate	$LiCoO_2$	1:0.9:2.1	–

scattering cross section is non-Rutherford in nature. As a result, the accuracy of p-EBS depends, in addition to the factors applicable to RBS, on the accuracy of the experimentally or theoretically determined scattering cross-sections as well. Therefore the accuracy of the differential cross-sections of ^{6}Li(p,p)^{6}Li, ^{7}Li(p,p)^{7}Li, and O(p,p)O scattering and the assumption that scattering cross-sections for Ti and Co are entirely Rutherford may be among the factors behind the discrepancy in the compositions determined by p-EBS. The present method, however, does not suffer from such limitation and, therefore, can be considered to be superior to p-EBS. It is, in fact, superior even to the PIGE method described in Ref. [11] (which is performed with 8 MeV protons and is susceptible to interference from fluorine) and thus is the preferred choice for the complete compositional analysis of titanate and cobaltate ceramics. Furthermore, it is instructive to mention that due to the sensitivity of PIGE to Cr and Mn, the methodology can be extended to the analysis of $LiCrO_4$ and $LiMn_2O_4$ which are also important energy materials.

In order to further probe the potential of the method, it was applied to multinary compounds such as $LiFePO_4$ and $LiFePO_4$/C which, understandably, are analytically more complex and challenging than the titanates. $LiFePO_4$ and its composite with carbon (i.e. $LiFePO_4$/C) are promising cathode materials for Li-ion batteries. Figure 7 shows the PIGE spectrum of $LiFePO_4$ acquired with 4.0 MeV protons wherein the peaks of the constituent elements are vividly present. However, two features of the spectrum need special mention. Firstly, the signal of oxygen is relatively weak since it is riding over the Compton edge of 2230 keV γ-rays emitted from the ^{31}P(p, γ)^{32}S reaction. Secondly, the γ-peak at 843 keV, attributable to Fe, is unusually broad and consists of a shoulder around about 837 keV. The origin of the 837 keV γ-rays lies in the ^{73}Ge(n,γ)^{74}Ge and ^{72}Ge(n,n′γ)^{72}Ge reactions taking place in the Ge crystal of the HPGe detector [27] while the neutrons involved in inducing these reactions are produced from the ^{7}Li(p,n)^{7}Be reaction (Q = − 1.664 MeV) occurring in the $LiFePO_4$ target. Therefore, the true contribution of Fe was determined by fitting the envelope around 843 keV into two components. Meanwhile, the content of carbon in the $LiFePO_4$/C composite specimen was determined by means of the ^{13}C(p,p′γ)^{13}C reaction that emits 3089 keV γ-rays [28]. The compositions of the compounds thus measured are listed in Table 4. The combined uncertainty of the

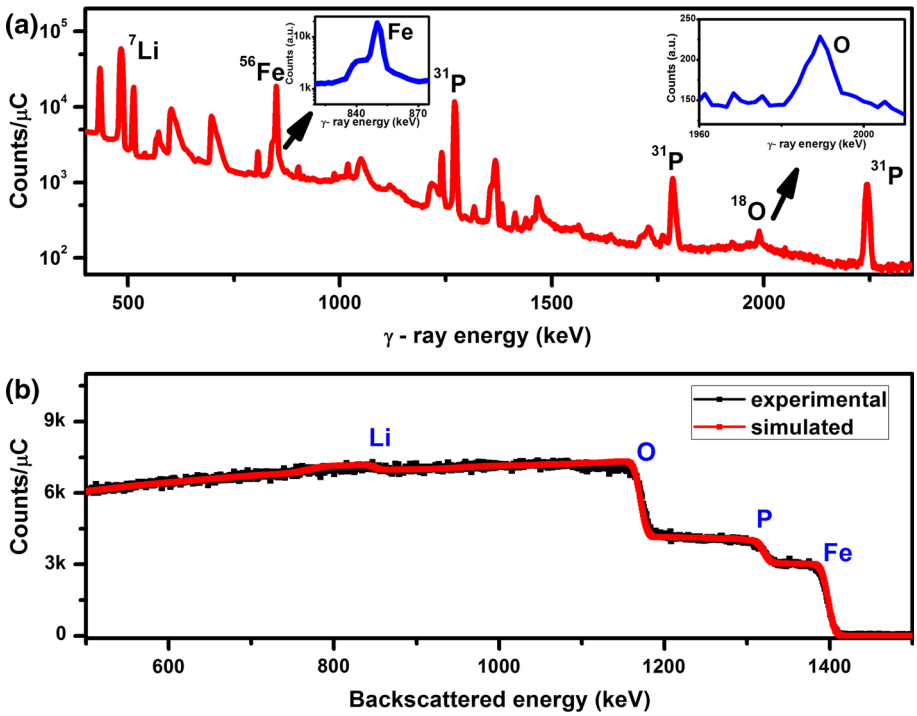

Fig. 7 Analysis of $LiFePO_4$: **a** a PIGE spectrum and **b** a proton backscattered spectrum recorded with 4.0 and 1.5 MeV protons respectively. The insets in Fig. **a** show the peaks of Fe and oxygen

Table 4 Atomic composition of different quaternary oxides determined by PIGE and p-EBS

Chemical formula	Determined [Li:Fe:P:O(C)]	
	PIGE	p-EBS
$LiFePO_4$	1:1:0.9:3.6	1:0.9:0.8:3.4
$LiFePO_4$/C	1:1.2:0.8:4.4 (1.9)	1:1.1:1.1:4.6 (2.2)

analysis which has contributions from the peak area measurement, the stopping cross section and the charge integration of the sample as well as the standard is estimated to be about 5% for the binary and about 8% for the quaternary or multinary compounds. In fact, standardless PIGE measurements can provide results with much better uncertainty, however, it requires a precise knowledge of reaction cross-sections over a wide range of proton energy, the efficiency of the detector for γ-rays of different energies and other parameters appearing in the equation relating the yield of the γ-rays with the concentration of the elements [29].

For the sake of cross-validation, the multinary compounds were also analysed by proton backscattering spectrometry with a typical backscattered spectrum of $LiFePO_4$ shown in Fig. 7(b). Though the signal (step) of Fe, P or O is prominent, that of Li is not as prominent as in the spectrum of $Li_2Ti_2O_4$ in Fig. 6(b) due to its comparatively lower content in the compound and relatively higher background. An examination of the data presented in Table 4 shows that for $LiFePO_4$ the PIGE and p-EBS results are in good agreement but for $LiFePO_4$/C, a disagreement in values for Fe and, particularly for P prevails which, apart from the uncertainty associated with the differential scattering cross-sections of the different isotopes, may also arise due to the inhomogeneous distribution of the elements. It is to be noted that as compared to the probing depth of tens of microns of PIGE with 4.0 MeV protons, EBS performed with 1.5 MeV protons has a probing depth of only about 8 micron in $LiFePO_4$. These considerations suggest that PIGE provides a more effective approach for the compositional analysis of this important class of materials.

Conclusions

The $^{18}O(p,p'\gamma)^{18}O$ nuclear reaction emitting 1982 keV γ-rays is employed in PIGE measurements for the determination of bulk oxygen in materials. The method is simple, rapid and non-destructive. It is endowed with a detection limit of $\sim$ 2 at% in heavy matrices and $\geq$ 15 at% in light matrices, and has a probing depth of more than 30 μm at the 4.2 MeV proton energy. High precision measurement of oxygen in mid and high Z matrices is one of the discerning features of the method. It can, therefore, be applied to determine subtle changes in the oxygen stoichiometry in such materials. The method is largely free from nuclear or spectral interferences. However, due to the higher sensitivity of PIGE to low Z elements such as Li, B, Na, Al etc.,

the presence of these elements in high abundance can impair its detection limit and rapidity. Nevertheless, the simultaneous multielement detection capability of the technique can be exploited to determine the complete elemental composition of such compounds. It is amply demonstrated by analyzing complex oxides such as Li_2TiO_3 and $LiFePO_4$. Finally, though not probed explicitly, the simultaneous occurrence of the $^{16}O(p,\gamma)^{17}F$, $^{17}O(p,p'\gamma)^{17}O$ and $^{18}O(p,p'\gamma)^{18}O$ nuclear reactions emitting 495, 871 and 1982 keV γ-rays raises the possibility of isotopic analyses of oxygen in favourable materials.

Acknowledgements The authors gratefully acknowledge the useful comments and suggestions of Dr. P. D. Naik, Associate Director, Chemistry Group, BARC and Dr. Sunil Jai Kumar, Head, NCCCM, Hyderabad. The authors thank Prof. C. Sudakar for providing $LiFePO_4$ and $LiFePO_4$/C samples.

References

1. Zheng J, Xiao J, Zhang Ji-Guang (2016) The roles of oxygen non-stoichiometry on the electrochemical properties of oxide-based cathode materials. Nano Today 11:678–694
2. Ganduglia-Pirovano MV, Hofmann A, Sauer J (2007) Oxygen vacancies in transition metal and rare earth oxides: current state of understanding and remaining challenges. Surf Sci Rep 62:219–270
3. Cohen DD, Rose EK (1992) Analysis of oxygen by charged particle bombardment. Nucl Instr Meth B 66:158–190
4. Amsel G, Samuel D (1967) Microanalysis of the stable isotopes of oxygen by means of nuclear reactions. Anal Chem 39(14):1689–1698
5. Csedreki L, Huszank R (2015) Application of PIGE, BS and NRA techniques to oxygen profiling in steel joints using deuteron beam. Nucl Instr Meth B 348:165–169
6. Luomajarvi M, Rauhala E, Hautala M (1992) Oxygen detection by non-Rutherford backscattering below 2.5 MeV. Nucl Instr Meth B 9:255–258
7. Leavitt JA, McIntyre LC Jr, Ashbaugh MD, Oder JG, Lin Z, Dezfouly-Arjomandy B (1990) Cross sections for 170.5° backscattering of ^{4}He from oxygen for ^{4}He energies between 1.8 and 5.0 MeV. Nucl Instr Meth B 44:260–265
8. Vickridge IC, Tallon J, Presland M (1994) High precision determination of ^{16}0 in high T_c superconductors by DIGME. Nucl Instr Meth B 85:95–99
9. Vickridge IC, Tallon J, Presland M (1995) ^{16}O DIGME of high T_c materials. Nucl Instr Meth B 99:450–453
10. Raisanen J (1986) A rapid method for carbon and oxygen determination with external proton induced gamma-ray emission analysis. Nucl Instr Meth B 17:344–348
11. Chhillar S, Acharya R, Tripathi R, Sodaye S, Sudarshan K, Rout PC, Mukerjee SK, Pujari PK (2015) Compositional characterization of lithium titanate ceramic samples by determining Li, Ti and O concentrations simultaneously using PIGE at 8 MeV proton beam. J Radioanal Nucl Chem 305(2):463–467
12. Kumar S, Sunitha Y, Reddy GLN, Sukumar AA, Ramana JV, Sarkar A, Verma R (2016) Oxygen determination in materials by 18O(p,αγ)15 N nuclear reaction. Nucl Instr Meth B 378:38–44
13. Kiss AZ, Koltay E, Nyako B, Somorjai E, Anttila A, Raisanen J (1985) Measurements of relative thick target yields for PIGE analysis on light elements in the proton energy interval 2.4–4.2 MeV. J Radioanal Nucl Chem 89:123–141
14. Mateus R, Jesus AP, Ribeiro JP (2005) A code for quantitative analysis of light elements in thick samples by PIGE. Nucl Instr Meth B 229:302–308
15. Ziegler JF, Biersack JP, Ziegler D (2013) SRIM- The Stopping and Range of Ions in Matter. http://www.srim.org/
16. Mayer M (1997) SIMNRA user's guide, Report IPP 9/113. Max Planck Institute for Plasmaphysik, Garching, Germany
17. Bashkin S, Richards HT (1951) Proton bombardment of the lithium isotopes. Phys Rev 84:1124–1129
18. Malmberg PR (1956) Elastic scattering of protons from Li^7. Phys Rev 101:114–117
19. Gurbich AF (1998) Evaluation of non-Rutherford proton elastic scattering for cross section carbon. Nucl Instr Meth B 136–138:60–65
20. Gurbich AF (1997) Evaluation of non-Rutherford proton elastic scattering for cross section oxygen. Nucl Instr Meth B 129:311–316
21. Ajzenberg-Selove F (1986) Energy levels of light nuclei $A = 16$–17. Nucl Phys A 460(1):1–110
22. Ajzenberg-Selove F (1987) Energy levels of light nuclei A = 18–20. Nucl Phys A 475(1):1–198
23. Sunitha Y, Kumar Sanjiv (2017) Depth profiling Li in electrode materials of lithium ion battery by ^{7}Li(p, γ)^{8}Be and ^{7}Li(p, α)^{4}He nuclear reactions. Nucl Instr Meth B 400:22–30
24. Rauhala E, Keinonen J (1988) Ion beam analysis of oxygen distribution in superconducting $YBa_2Cu_3O_x$. Appl Phys Lett 52:1520–1522
25. Habrioux A, Surblé S, Berger P, Khodja H, D'Affroux A, Mailley S, Gutel T, Patoux S (2012) Nuclear microanalysis of lithium dispersion in $LiFePO_4$ based cathode materials. Nucl Instr Meth B 290:13–18
26. Colaux JL, Jeynes C, Heasman KC, Gwilliam RM (2015) Certified ion implantation fluence by high accuracy RBS. Analyst 140:3251–3261
27. Fehrenbacher G, Meckbach R, Paretzke HG (1996) Fast neutron detection with germanium detectors: computation of response functions for the 692 keV inelastic scattering peak. Nucl Instr Meth A 372:239–245
28. Sunitha Y, Kumar Sanjiv (2017) ^{10}B/^{11}B isotopic ratio and atomic composition of boron carbide: determination by proton induced γ-ray emission and proton elastic backscattering spectrometry. Appl Radiat Isot 128:28–35
29. Mateus R, Jesus AP, Braizinha B, Cruz J, Pinto JV, Ribeiro JP (2002) Proton-induced γ-ray analysis of lithium in thick samples. Nucl Instr Meth B 190:117–121